M. Goldman, L. Tabarovsky and M. Rabinovich

INTERPRETATION OF 2.5-D TRANSIENT ELECTROMAGNETIC DATA IN TERMS OF 1-D HORIZONTALLY LAYERED EARTH.

INTRODUCTION

The most convential interpretation model used in Transient Electromagnetic (TEM) sounding methods is a one-dimensional (1-D) horizontally layered earth. Although the 1-D interpretation has proved feasible in many practical cases, significant inaccuracies may occur when true geoelectrical structures are essentially multi-dimensional. In this case the use of an appropriate multi-dimensional inversion scheme would be the most useful. Unfortunately at present the latter is not available for TEM soundings, although isolated 3-D trial-and-error interpretation attempts were made recently (Hördt et al., 1992; Strack, 1992). In any case, a crucial point for either future 3-D inversion or, especially, the current trial-and-error 3-D interpretation, would be the correct choice of starting model. The latter requires a better understanding of the multi-dimensional effects on the data acquired. These effects can be examined either directly from appropriate forward solutions (Gunderson et al., 1986) or by applying 1-D inversion to multi-dimensional data (Goldman and Stoyer, 1983; Newman et al., 1986). We used the second approach, since it permits evaluation of the limitations of 1-D interpretation widely used in practice.

The forward solution used in our investigation belongs to the so-called quasi-three-dimensional (Q3D) problems (arbitrary source, axially-symmetrical earth model, Fig. 1). From the computational point of view, these problems are in fact 2.5-D problems, i.e. they are far more computationally efficient than 3-D problems proper. On the other hand, contrary to standard 2.5-D problems which involve infinitely long structures, the axially symmetrical bodies (sphereoids, finite cylinders, etc.) are essentially three-dimensional and, in many cases, simulate real 3-D geoelectric structures with the same degree of reliability as traditional 3-D prisms or any other regular geometrical bodies. Moreover, comparison of our Q3D calculations for a finite circular cylinder with standard 3-D modeling for a prismatic body having appropriate geometrical parameters (Anderson and Newman, 1985) showed that, in many cases, the responses are similar if not identical (Fig. 2 and 3).

FORWARD SOLUTION

The finite-difference (FD) algorithm to calculate the transient response for the model shown in Figure 1 directly in the time domain, has been developed and described in detail by Tabarovsky and Rabinovich (1988). A brief summary of the most important features of the algorithm used can be formulated as follows:

- The solution is sought for the Hertz potential of an electrical type. Using axial symmetry of the model the latter can be represented as Fourier series with respect to angular harmonics. The FD algorithm is applied then to the 2-D amplitudes of the Fourier series.

- Further simplification is done by introducing auxiliary scalar potentials, which allow to reduce the original vectorial equation to only three independent scalar equations. However, the boundary conditions for the scalar potentials turn out to be mixed and this problem is treated numerically by choosing the proper succession in the application of the FD algorithm.

- In order to simplify the FD algorithm in the vicinity of the source, the solution is sought for the secondary potentials.

- In order to exclude the uppermost halfspace (air) from consideration a special boundary condition at the earth's surface (integral-differential equation) is formulated.

- Due to the complicated boundary conditions, the FD algorithm is conditionally stable; in order to provide its stability both spatial and temporal discretization intervals must decrease as the resistivity contrast between the body and the surrounding medium increases.

1-D INVERSION OF 2.5-D SYNTHETIC DATA

The synthetic data calculated were interpreted in terms of one-dimensional, horizontally layered models. In addition to the analysis of the influence of 3-D effects in a 1-D interpretation, an attempt was made to develop simple correction procedures which would allow recovery of 3-D structures with reasonable accuracy by using only the data collected and by doing 1-D inversions along the profile.

In order to reduce the number of model parameters without essentially reducing the generality of the problem, the model shown in Figure 1 was significantly simplified. The number of layers in the host medium was set at two, while the body, having the resistivity of either the upper layer or of the basement, formed either a depression or a high respectively (Figure 4). This led not only to a significant simplification of the inversion procedure, but, and what is most important, also avoided an almost inevitable non-uniqueness in the interpretation of the layered earth parameters playing a role.

The following two most popular transmitter/receiver (T/R) configurations are considered:

1. central loop configuration, the favorite array for the so-called short offset modification of the TEM method (SHOTEM); and
2. fixed grounded wire/moving vertical magnetic dipole, the most widely used array in the long offset (LOTEM) modification of TEM soundings.

The main results of the conducted investigation can be briefly formulated as follows:

- 3-D structures in the form of the basement high and depression can be recovered with reasonable accuracy using central loop soundings along a profile and applying 1-D inversion to each set of sounding data (Fig. 5 and 6). The application of 1-D inversion to fixed transmitter/moving receiver data would mean missing the structural depressions completely and would lead to much greater errors in recovery of the structural highs (Fig. 7 and 8).

- The main misleading factor in 1-D interpretation of significantly 3-D data is the appearance of fictitious layers in the vicinity of the vertical boundaries. This problem can be handled in various ways depending on the 3-D geometry and resistivity contrasts.

1 A Structural Depression in a Resistive Basement

The right ascending branch of the apparent resistivity curve is more steeply inclined than is theoretically possible for any 1-D model having even an infinitely resistive basement. The problem is solved by introducing a fictitious, extremely high conductive basement which is further excluded from consideration (Fig. 5b). This procedure is not misleading since the absolute resistivity value of the fictitious basement is far beyond any known real resistivity values.

2 Structural Depression in a Conductive Basement

The appearance of the fictitious layers changes the type of the apparent resistivity curves: the latter become Q-type, 3-layer curves. In order to recover the structure it is proposed that those two layers which have a lesser resistivity contrast be combined (Fig. 5a). This procedure can be somewhat misleading in the case of an individual sounding, but it should not cause any difficulties in the interpretation of the data along the whole profile.

The important common feature of the corrected interpretation for both models is that all resistivities are obtained with reasonable accuracy, while the amplitude of the depression is essentially underestimated. However, since the latter feature is extremely consistent not only within the limits of the model considered, but for the other 3-D models as well (Newman et al., 1986), further corrections can be made for the amplitude of the depression.

3 Structural High in Both Resistive and Conductive Basements

In this case interpretation is far more complicated since two fictitious layers appear in the 1-D interpretation above the structure. In order to recover the structure, only the shallowest resistivity contrast is taken into account, while the deeper layers are combined in one, having the resistivity of the lowermost half space. In some cases the lateral resolution of the measurements can be improved if the absolute values of the resistivity contrasts are also taken into consideration. This can be done by excluding all relatively small resistivity contrasts leaving only the largest (Fig. 6a). These procedures are recommended if the structure is the only target of the survey, or if the model recovered will be used for further 3-D interpretation.

The resistivity of the upper layer and the amplitude of the structure are obtained with high accuracy. This conclusion coincides with the results of Newman et al. (1986), with the reservation that our 4-layer interpretation was practically unique.

In order to avoid any possible misunderstanding, it must be clearly emphasized that the above results and, in particular, recommendations must be applied if either no a priori information is available or if the correction procedures do not contradict the existing information. This is because we took the greatest care to avoid as far as possible an incorrect 1-D interpretation caused by 3-D effects rather than to obtain complete geological/geoelectrical information. In other words, the application of the proposed correction methods may lead to missing some existing objects rather than to the "discovery" of fictitious ones. It should be clear, however, that the probability of missing these features can be greatly diminished by using the information along the whole profile(s) and it can probably be reduced to zero by further application of 3-D inversion algorithms.

As far as comparison of central loop and fixed transmitter/moving receiver configurations is concerned, the latter is obviously much less efficient in mapping relatively deep confined structures. Although we restricted ourselves by considering only 1-D interpretation, this conclusion would appear to be valid in the general case, since it is based on different anomalous effects measured in both configurations. It should be emphasized, however, that much better resolution is expected in LOTEM surveys if they are properly designed, i.e. if, in addition to or instead of the conventional cost-effective fixed transmitter/moving receiver configuration, a more expensive but geophysically more efficient moving transmitter/moving receiver array is used.

ACKNOWLEDGEMENTS

Our thanks are due to Walt Anderson who provided us with the 3-D calculations used for the comparison and to Andreas Hördt for very fruitful discussions of the interpretational aspects of our research. We also thank Kurt Strack who critically read the manuscript and made numerous corrections, some of which we incorporated in revision.

REFERENCES

Anderson, W.L., and Newman, G.A., 1985. *An album of three-dimensional transient electromagnetic responses for the central-induction loop configuration.* U.S. Dept. of the Interior, Geological Survey Report 85-745.

Goldman, M.M., and Stoyer, C.H., 1983. Finite-difference calculations of the transient field of an axially symmetric earth for vertical magnetic dipole excitation, *Geophysics,* **48**, 953-963.

Gunderson, B.M., Newman, G.A., and Hohmann, G.W., 1986. Three-dimensional transient electromagnetic responses for a grounded source, *Geophysics*, **51**, 2117-2130.

Hördt, A., Druskin, V.L., Knizhnerman, L.A. and Strack, K.M., 1992. Interpretation of 3-D effects in long offset transient electromagnetic (LOTEM) soundings in the Munsterland area, Germany, *Geophysics,* **57**,

Interpex Limited, 1989, TEMIX User's Manual, Interpex Ltd., 142 pp.

Newman, G.A., Hohmann, G.W., and Anderson, W.L., 1986. Transient electromagnetic response of a three-dimensional body in a layered earth, *Geophysics,* **51**, 1608-1627.

Strack, K.M., 1992. *Exploration with deep transient electromagnetics.* Elsevier, Amsterdam.

Tabarovsky, L.A., and Rabinovich, M.B., 1988. *Mathematical modeling of transient electromagnetic fields in quasi-three-dimensional models.* VINITI, N6264-B88 (in Russian).

FIGURE CAPTIONS

Fig. 1 General model geometry.

Fig. 2 Model geometry used for comparison of 2.5-D and 3-D (Anderson and Newman, 1985) calculations.

Fig. 3 Comparison of 2.5-D (open diamonds) and 3-D (solid lines) voltage responses for the model shown in Fig. 2 (2.5-D calculations are carried out for the inner cylinder):

a) Receiver location $x = +600m$.

b) Receiver location $x = -1000m$.

Fig. 4 Model geometry used in the investigation.

Fig. 5 Results of 1-D inversion of 2.5-D central loop synthetic data.

a) The true resistitives are 300 Ohm-m for the upper layer and 10 Ohm-m for the basement.

b) The true resistivities are 10 Ohm-m for the upper layer and 300 Ohm-m for the basement.

Fig. 6 Results of 1-D inversion of 2.5-D central loop synthetic data.

a) The true resistivities are 300 Ohm-m for the upper layer and 10 Ohm-m for the basement. Dotted line shows the improved resolution (see text for details).

b) The true resistivities are 10 Ohm-m for the upper layer and 300 Ohm-m for the basement.

Fig. 7 Results of 1-D inversion of 2.5-D fixed transmitter/moving receiver synthetic data along the profile located behind the structure. The true resistivities are 300 Ohm-m for the upper layer and 10 Ohm-m for the basement.

Fig. 8 Results of 1-D inversion of 2.5-D fixed transmitter/moving receiver synthetic data along the profile located behind the structure. The true resistivities are 10 Ohm-m for the upper layer and 300 Ohm-m for the basement.

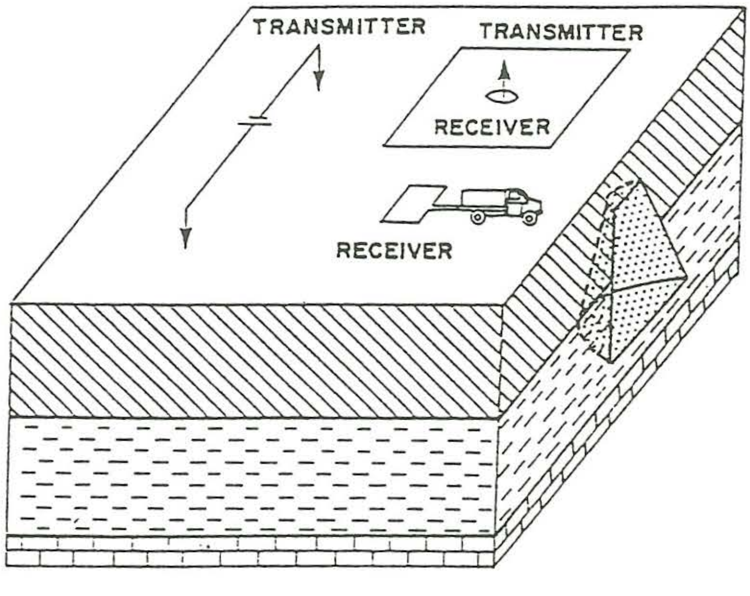

Fig. 1

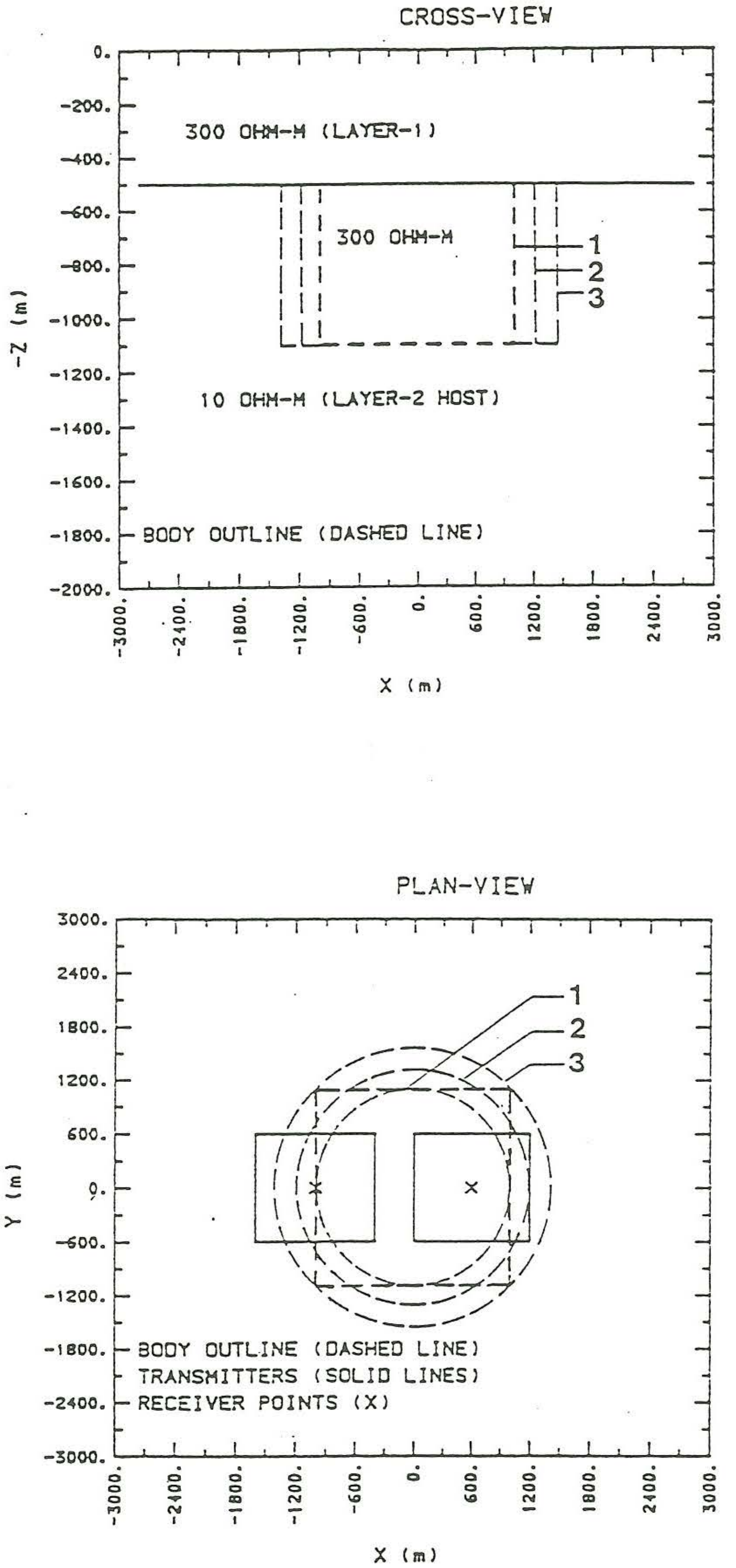
CROSS-VIEW
300 OHM-M (LAYER-1)
300 OHM-M
1
2
3
10 OHM-M (LAYER-2 HOST)
BODY OUTLINE (DASHED LINE)
-Z (m)
X (m)
PLAN-VIEW
1
2
3
BODY OUTLINE (DASHED LINE)
TRANSMITTERS (SOLID LINES)
RECEIVER POINTS (X)
Y (m)
X (m)

Fig. 2

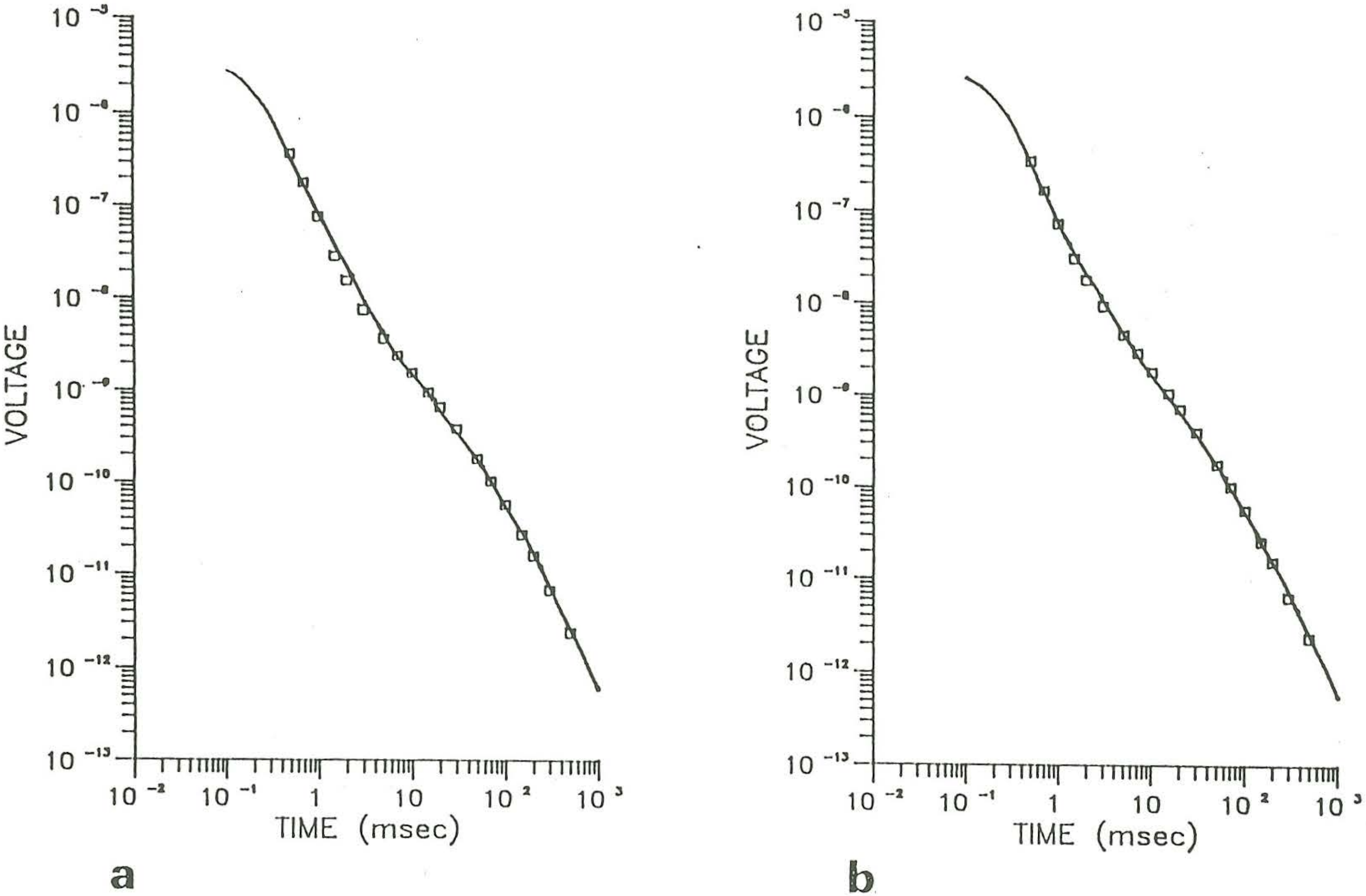

Fig. 3

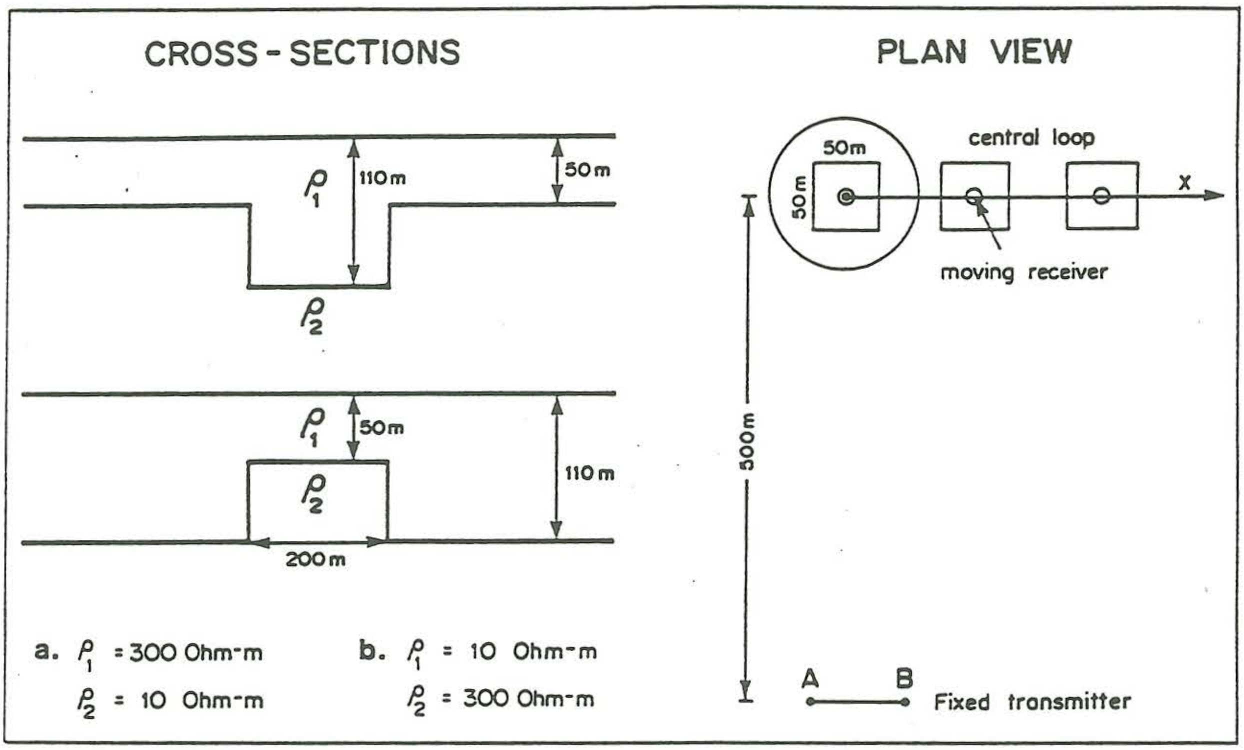

CROSS - SECTIONS
PLAN VIEW
110 m
50 m
50 m
110 m
200 m
a. ρ_1 = 300 Ohm-m
ρ_2 = 10 Ohm-m
b. ρ_1 = 10 Ohm-m
ρ_2 = 300 Ohm-m
50m
50m
central loop
X
moving receiver
500m
A
B
Fixed transmitter

Fig. 4

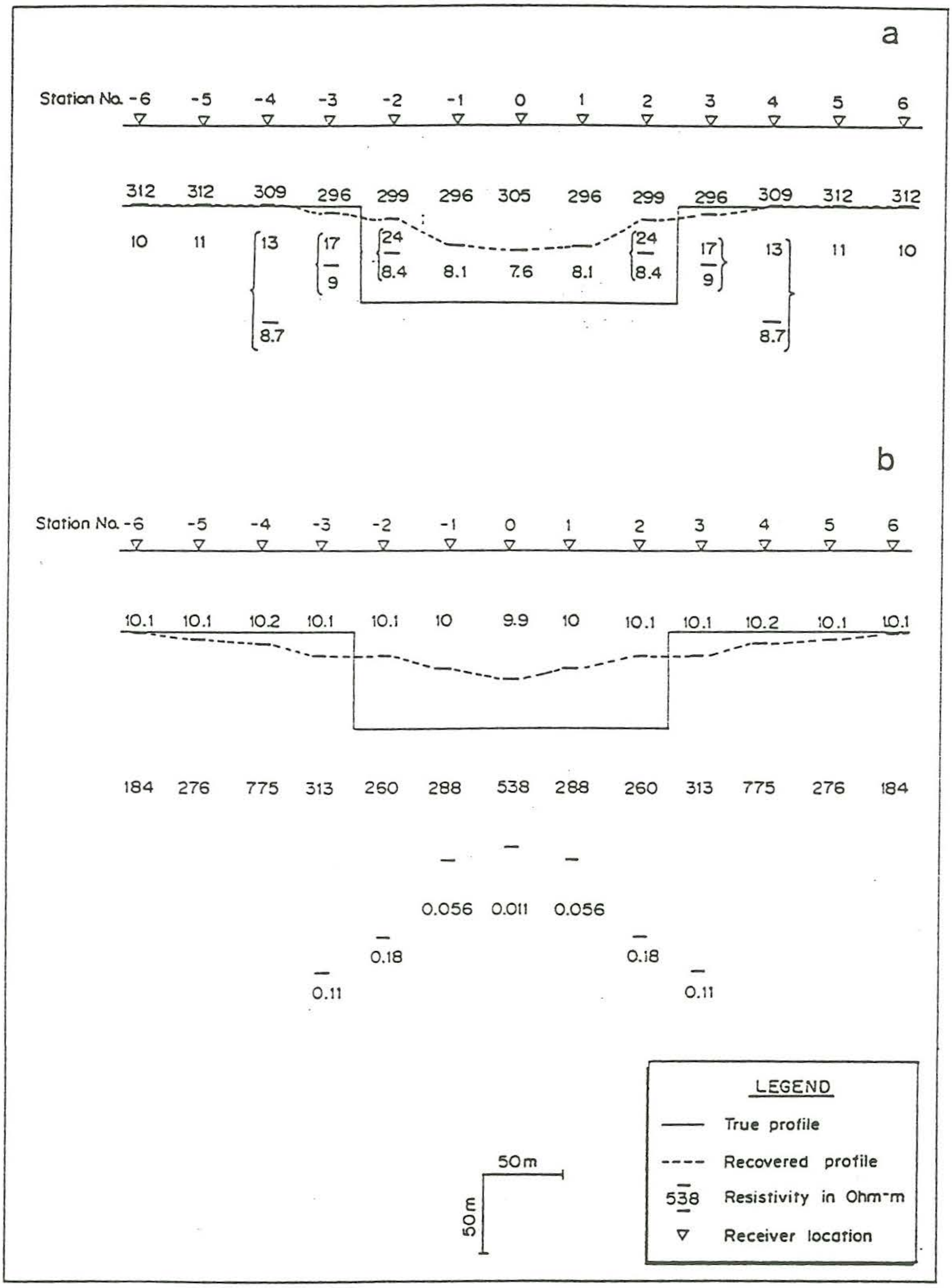
a
Station No. -6 -5 -4 -3 -2 -1 0 1 2 3 4 5 6
312 312 309 296 299 296 305 296 299 296 309 312 312
10 11 13 17 24 24 17 13 11 10
9 8.4 8.1 7.6 8.1 8.4 9
8.7 8.7
b
Station No. -6 -5 -4 -3 -2 -1 0 1 2 3 4 5 6
10.1 10.1 10.2 10.1 10.1 10 9.9 10 10.1 10.1 10.2 10.1 10.1
184 276 775 313 260 288 538 288 260 313 775 276 184
0.056 0.011 0.056
0.18 0.18
0.11 0.11
LEGEND
True profile
Recovered profile
538 Resistivity in Ohm-m
Receiver location
50m
50m

Fig. 5

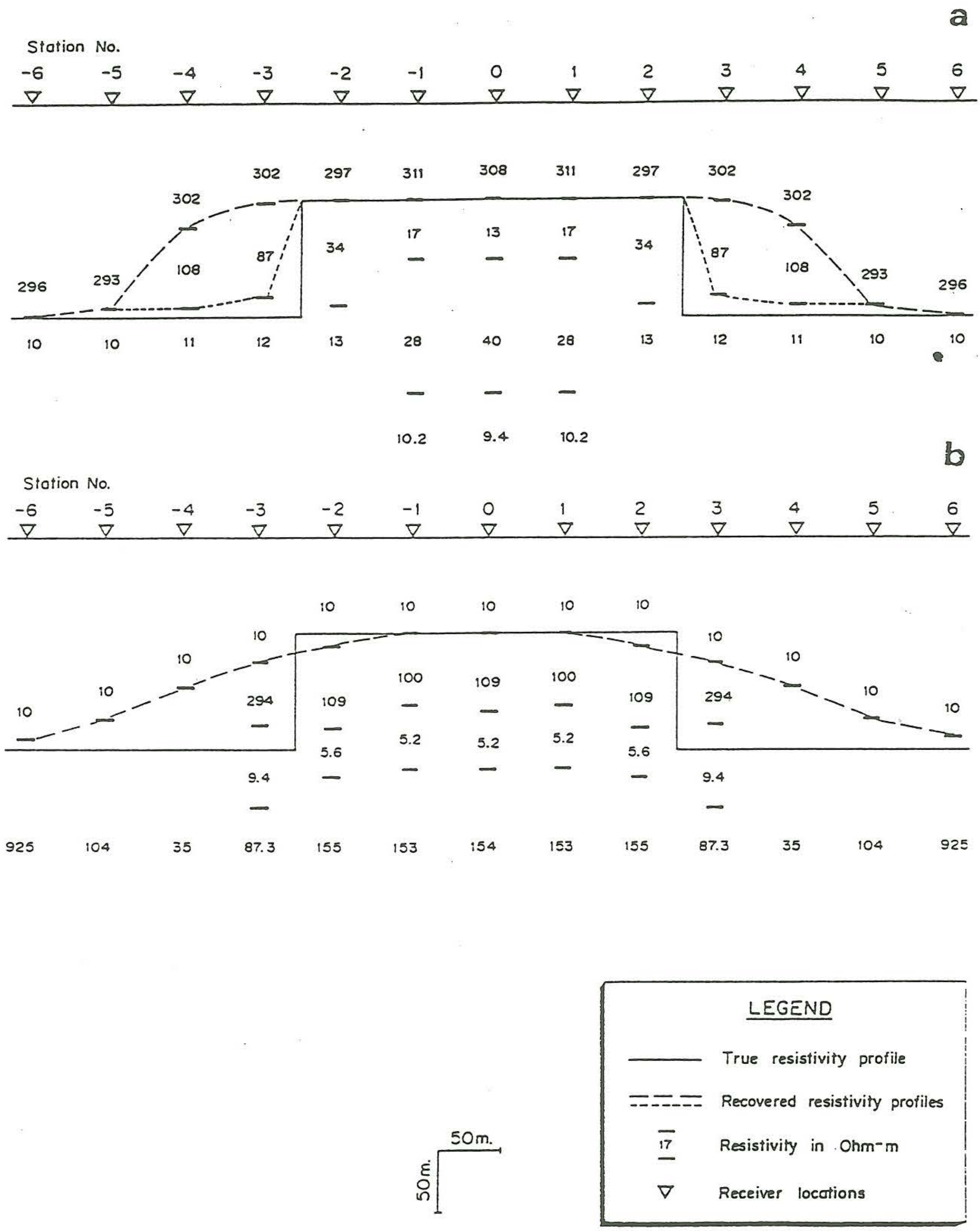
a
Station No.
-6 -5 -4 -3 -2 -1 0 1 2 3 4 5 6
302 297 311 308 311 297 302
302 302
17 13 17
34 34
87 87
108 108
296 293 293 296
10 10 11 12 13 28 40 28 13 12 11 10 10
10.2 9.4 10.2
b
Station No.
-6 -5 -4 -3 -2 -1 0 1 2 3 4 5 6
10 10 10 10 10
10 10
10 10
10 10
10 10
100 109 100
294 109 109 294
5.6 5.2 5.2 5.2 5.6
9.4 9.4
925 104 35 87.3 155 153 154 153 155 87.3 35 104 925
LEGEND
True resistivity profile
Recovered resistivity profiles
17 Resistivity in Ohm-m
Receiver locations
50m.
50m.

Fig. 6

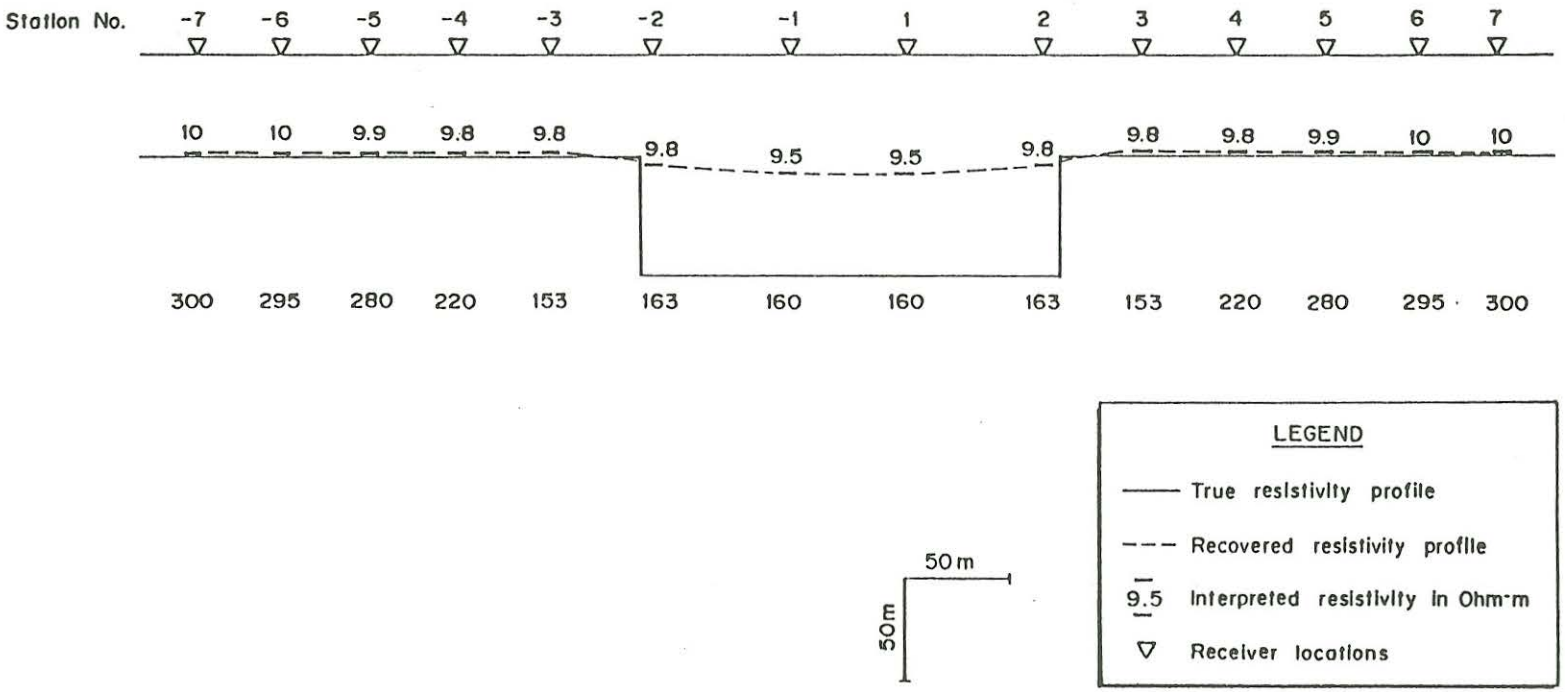

Station No.
-7 -6 -5 -4 -3 -2 -1 1 2 3 4 5 6 7
10 10 9.9 9.8 9.8 9.8 9.5 9.5 9.8 9.8 9.8 9.9 10 10
300 295 280 220 153 163 160 160 163 153 220 280 295 300
50 m
50m
LEGEND
True resistivity profile
Recovered resistivity profile
9.5 Interpreted resistivity in Ohm-m
Receiver locations

Fig. 7

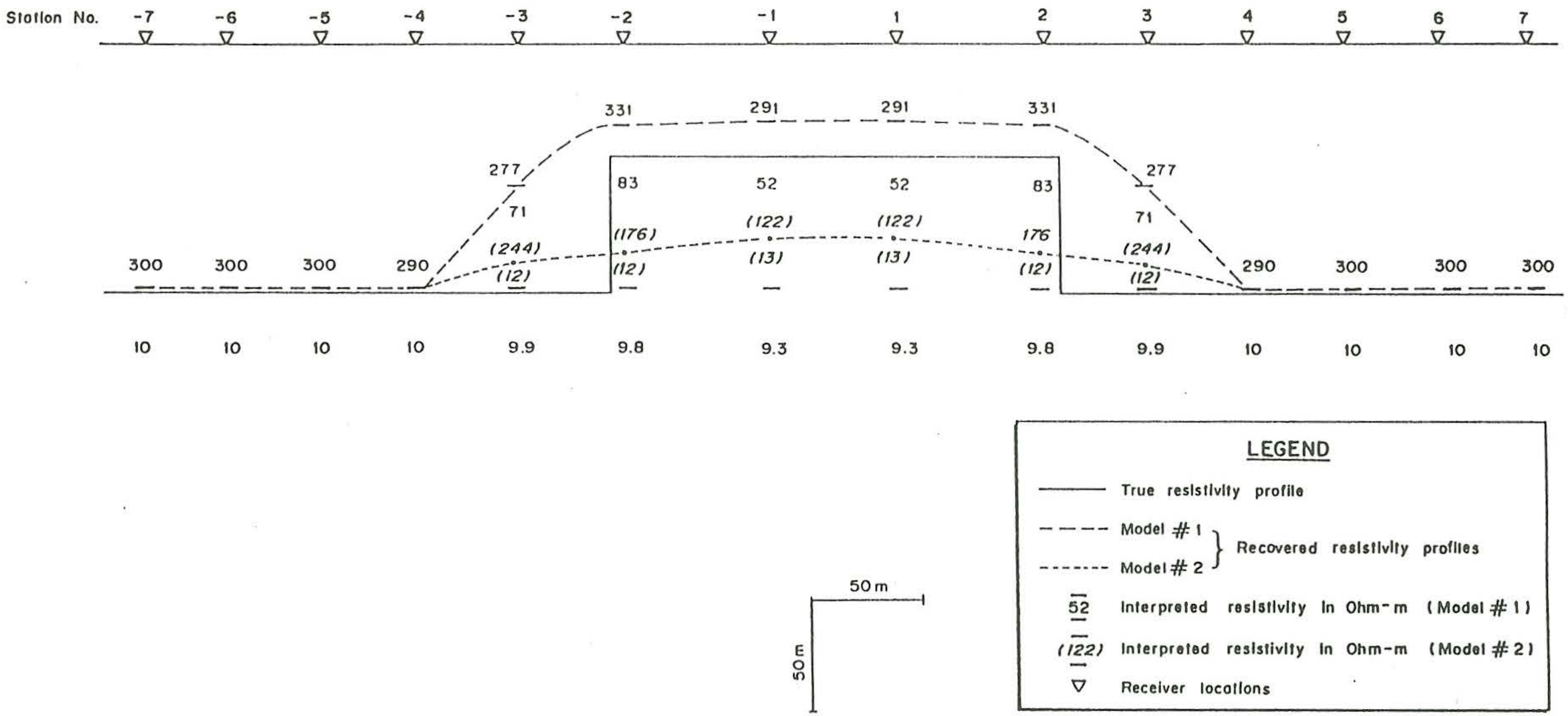
Station No.
-7 -6 -5 -4 -3 -2 -1 1 2 3 4 5 6 7
331 291 291 331
277 277
83 52 52 83
71 71
(176) (122) (122) 176
300 300 300 290 (244) (244) 290 300 300 300
(12) (12) (13) (13) (12) (12)
10 10 10 10 9.9 9.8 9.3 9.3 9.8 9.9 10 10 10 10
50 m
50 m
LEGEND
True resistivity profile
Model # 1
Model # 2
Recovered resistivity profiles
52 Interpreted resistivity in Ohm-m (Model # 1)
(122) Interpreted resistivity in Ohm-m (Model # 2)
Receiver locations

Fig. 8